

Hardness Perception by Tapping: Effect of Dynamic Stiffness of Objects

Kosuke Higashi¹, Shogo Okamoto¹, Yoji Yamada¹, Hikaru Nagano², and Masashi Konyo²

Abstract— Humans can judge the hardness of an object by tapping its surface using a fingertip. The damped natural vibration caused by tapping is a vibrotactile cue for hardness perception. We investigated how dynamic characteristics of an object or vibration influence the hardness perceived by tapping. Using multivariate analyses, the subjectively reported hardness was linked with the dynamic stiffness of an object. Dynamic stiffness, which characterizes the impulsive response of an object, was acquired across 40–1,000 Hz for fourteen types of material cuboid through a hammering test. These blocks were also ranked by seven participants based on their hardness perceived when the participants tapped them with a finger. It was found that the dynamic stiffness did not equally affect the hardness perception across the wide frequency range. Its sensitivity displayed a peak around 200–400 Hz and decreased or disappeared at greater frequency bands in which human perceptual capability is limited.

I. INTRODUCTION

In our daily lives, we tap an object's surface in order to judge its hardness properties when the object is rigid and cannot be deflected by pinching or pushing. Surprisingly, thus far, the principle of hardness perception by tapping has yet to be intensively studied. The general agreement among previous studies seems to be that the dominant frequency of the transient vibration yielded by tapping is a major cue for judging the hardness-related properties of objects [1], [2], [3], [4]. Greater frequencies lead to a greater perceived hardness. Other studies reported intriguing properties, although they still need to be retested and endorsed under various conditions by several studies before they can be widely accepted. For example, using vibrotactile display devices, artificially displaying multiple frequency components in a single tapping event produces quality hardness stimuli [2], [5]. The viscosity or the damping properties of objects may also determine the hardness perceived by tapping as well as the stiffness of objects [6]. Although we focus on vibrotactile cueing in the present study, we should mention that the force cue, the rising steepness of the reaction force against an impulsive force input, likely significantly influences the hardness perceived by striking an object [7], [8], [9]. In spite of these previous attempts, few researchers have studied the vibrational frequency characteristics associated with the hardness perceived by tapping.

In previous studies using force or vibrotactile displays to virtually present the tapping event based on a transient vibration, vibratory stimuli tended to be simplified to damped

This study was partly supported by JSPS Kakenhi (15H05923) and ImPACT (Tough Robotics Challenge).

¹Department of Mechanical and Aerospace Engineering, Nagoya University, Nagoya, Japan. ²Graduate School of Information Sciences, Tohoku University, Sendai, Japan.

vibrations including a single frequency component. However, in reality, the response of an object against an impulsive tapping force includes a wide range of frequency components. In the present study, we investigate the perceptual effects of wide-frequency characteristics of 40–1,000 Hz on the hardness perception. To this end, we used the dynamic stiffness of the object. Dynamic stiffness is the force per unit vibratory displacement and is defined in the frequency domain. The transient vibration caused by tapping an object is mathematically decoupled into an impulsive force input by tapping and the dynamic stiffness unique to that object. Hence, the dynamic stiffness expresses the unique frequency characteristics associated with the hardness of the object. We linked the dynamic stiffness and subjective hardness of objects by multivariate analysis and determined the contribution of the dynamic stiffness for each frequency band. The dynamic stiffness was investigated by performing a mechanical test using an impulse hammer, and the subjective hardness was determined by subjecting the participants to a psychophysical test.

II. HARDNESS SPECIMENS

Fourteen types of specimens made of different materials were used in both mechanical and subjective tests. Each specimen is a solid block made of one of the fourteen types of materials listed in Table I. The blocks were comprised of plastic, wood, metal, rubber, and stone, which are popular materials in our daily lives. All materials were rigid enough not to be deflected when their surfaces were pushed with a fingertip. It should be noted that the dynamic stiffness of the object depends on the material and dimensions of the block. Hence, we did not purely investigate the differences in terms of materials. It is also true that both the material and structure of the object influence the softness perceived by pinching or pushing it [10].

III. PSYCHOPHYSICAL EXPERIMENT FOR SUBJECTIVE RATING OF HARDNESS SPECIMENS

A. Participants

The participants were seven male university students who agreed and provided informed consent. All of the participants were in their 20s and all were right-handed.

B. Procedures: Ranking task

Fourteen types of hardness specimens were randomly placed on a desk. The participants compared and ranked them by tapping their surfaces. The participants were instructed to tap the center of the largest area of each specimen using the index finger of their writing hand. To avoid judgment based

TABLE I
MATERIAL AND SIZE OF HARDNESS SPECIMENS

Material	Size [mm]
Acrylic resin	60 × 60 × 30
Polycarbonate resin	60 × 60 × 30
Nylon resin	60 × 60 × 30
Nitrile rubber	60 × 60 × 30
Urethane rubber (Soft)	60 × 60 × 30
Urethane rubber (Hard)	60 × 60 × 30
Wood	60 × 60 × 30
Wax	60 × 60 × 30
Stainless steel	60 × 60 × 30
Aluminum	60 × 60 × 30
Granite	100 × 100 × 30
Brick	100 × 100 × 60
Concrete	200 × 100 × 60
Cork	200 × 100 × 60

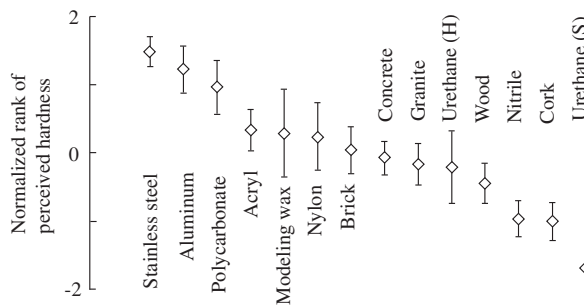


Fig. 1. Perceived hardness of specimens. Mean and standard deviations of normalized ranks among the participants.

on the surface texture or thermal properties, placing a finger on the specimen or pushing was not allowed. The number of taps was not specified and a participant could assign the same ranks to multiple specimens (i.e., multiple specimens could be perceived to have the same hardness). During the experiment, the participants wore headphones that played a pink noise to shutout the sounds of tapping. Furthermore, since sunglasses with opaque films were worn by the participants, judgment based on the appearance of the specimen was impossible. Note that the specimen blocks could barely be seen through the glasses. Most of the participants were able to finish the ranking task within 10 min.

C. Analysis of ranking data

For a better application of multivariate analyses described below, we converted the rank of each specimen assigned by individual participants into an interval scale using a normalized ranking method [11].

D. Results

Fig. 1 shows the mean and standard deviation of the normalized ranking scores for each specimen. The metal blocks were ranked highest, followed by plastic, stone, wood, and rubber. The hardness ranks were largely consistent with intuitive understanding, and irregularity was not observed. In the latter analysis, the mean scores were used as representative subjective hardness values.

IV. HAMMERING TEST FOR DETERMINING DYNAMIC STIFFNESS

A. Theory and analysis

The dynamic stiffness of an object is defined by the ratio of the force acting on the object $f(t)$ and its surface displacement $x(t)$ in the frequency domain. Given that we used an accelerometer to measure the surface vibration, the dynamic stiffness of the object is determined by

$$H(\omega) = \frac{\mathcal{F}[f(t)]}{\mathcal{F}[x(t)]} = \frac{\mathcal{F}[f(t)]}{\mathcal{F}[\ddot{x}(t)]/(j\omega)^2} \quad (1)$$

where \mathcal{F} and ω denote Fourier transform and the angular frequency, respectively. As described below, $\ddot{x}(t)$ and $f(t)$ were measured by an accelerometer fixed to the specimen surface and a load cell installed on an impulse hammer, respectively. Both types of values were then transformed into the values in the frequency domain using Fourier transform. Finally, we computed the absolute value of the ratio of the force to the displacement as the dynamic stiffness. For each specimen, the dynamic stiffness was averaged from the data acquired from ten hammer strikes. Taking into account the capabilities of the accelerometer that we used and human perception, we used the stiffness across 40–1,000 Hz for later analysis.

B. Experimental setup

Fig. 2 shows the measurement apparatus of the hammering test. An impulse hammer (GK-3100, Ono Sokki Co. Ltd., Japan) and a force amplifier (480M96A, Ono Sokki Co. Ltd.) intended for the load cell embedded in the hammer were used. A high-precision piezo accelerometer (2302B, Showa Sokki Co. Ltd., Japan, valid over 20 Hz) was fixed near the center of the surface that was to be struck by the hammer, and its output was acquired through an amplifier (4035-50, Showa Sokki Co. Ltd., Japan). The force and acceleration data were sampled using an oscilloscope at 10 kHz. Each specimen was fixed on a large metal plate (800 × 800 × 100 mm) for the hammering test.

The frequency response of the end tip of the hammer should ideally be similar to that of the human fingertip. Few end tips are commercially available for the impulse hammer we used. Among them, we chose the one whose frequency characteristics are most similar to those of the human fingertip. Fig. 3 shows the frequency spectrum of the impulsive force when the end tip or fingertip was used. Both responses agree fairly well with each other.

C. Procedure of hammering test

Each specimen was struck by the hammer at the center of its largest surface. Furthermore, each of the specimens was tested multiple times such that ten valid data values were acquired. Most common invalid trials were due to non-impulsive strikes with double hammering or a contact period that was too long. These invalid trials were easily detected by checking the force records. Fig. 4 shows an example of the force and acceleration acquired during a valid strike. The contact period of valid trials was generally 2–3 ms.

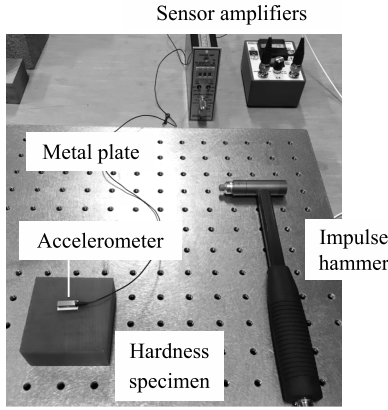


Fig. 2. Measurement apparatus for the hammering test

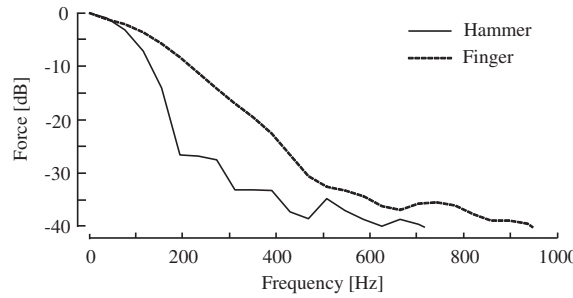


Fig. 3. Spectra of force impulses using a hammer and fingertip

D. Results: Dynamic stiffness of hardness specimens

Fig. 5 shows the dynamic stiffness computed for each of the fourteen specimens. The dynamic stiffness values agree with our intuitive understanding of hardness. The specimens composed of materials that we typically perceive as hard including, aluminum, stainless steel, concrete, and polycarbonate, displayed a relatively large stiffness value across the wide frequency range. In contrast, those composed of the soft materials, including urethane rubber, nitrile rubber, cork, and wood, were found to display less stiffness. The peak stiffness values differed for each of specimens, especially for softer materials. However, hard materials displayed similar dynamic stiffness values in the low frequency range.

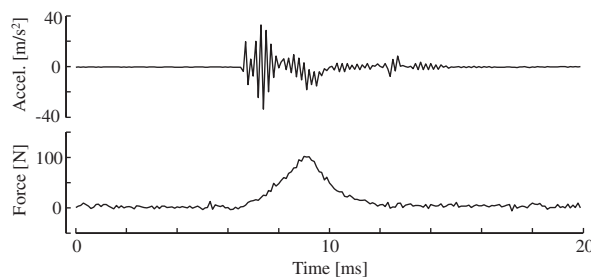


Fig. 4. Example of acceleration and force data acquired by performing a hammering test (Hard urethane)

V. LINKAGE OF DYNAMIC STIFFNESS AND PERCEIVED HARDNESS BY MULTIVARIATE ANALYSIS

A. Multivariate model and strategy of analysis

Based on the fact that the frequency of the damped vibration at the tapping event influences the perceived hardness [1], [2], [3], [5] and the perception of vibrotactile stimulus highly depends on its frequency [12], we linked the dynamic stiffness values $s_i \in \mathbb{R}^{n \times 1}$ of n representative frequencies for an object i and its normalized hardness rank h_i by

$$\begin{aligned} h_i &= s_i^T w + c \\ &= \sum_j^n s_{ij} w_j + c. \end{aligned} \quad (2)$$

where s_{ij} and w_j were the stiffness value at the j th representative frequency for object i and its perceptual weight, respectively. For m samples of dynamic stiffness, the regression model is

$$h = S w + c. \quad (3)$$

where $S = [s_1, s_2, \dots, s_m]^T$, $h = [h_1, h_2, \dots, h_m]^T$, and c are the matrix of dynamic stiffness, the vector of hardness scores, and a constant value that represents the intercept of hardness scores, respectively. Because of the collinearity among the explanatory variables, (3) cannot be directly solved by multiple regression analysis using the generalized inverse matrix of S . To avoid this issue, using principal component analysis, we factorized S into a few independent vectors before resolving (3) using those vectors.

B. Principal component analysis of dynamic stiffness

We computed the principal components of the dynamic stiffness of the fourteen types of specimens. Matrix $S \in \mathbb{R}^{m \times n}$ was composed of the stiffness values at n representative frequencies for m hammering test trials. Twenty-six points within 40 to 1,000 Hz were used as representative frequencies with the equal interval of 40 Hz: $n = 26$. The hammering test included 140 (14 types of specimens \times 10 trials) trials: $m = 140$. With a varimax rotation applied, S was decomposed into the component scores $A \in \mathbb{R}^{m \times n'}$ of all trials and the principal component vectors $B \in \mathbb{R}^{n' \times n}$ by

$$S = AB \quad (4)$$

where $n' < n$. The number of principal components was determined to be three such that the cumulative contribution ratio reached 95%: $n' = 3$.

C. Multiple regression analysis between hardness scores and dynamic stiffness using the reduced set of explanatory variables

We applied a multiple regression analysis with the principal component scores and subjective hardness scores being explanatory and objective variables, respectively. For this analysis, the subjective hardness scores h was modeled to

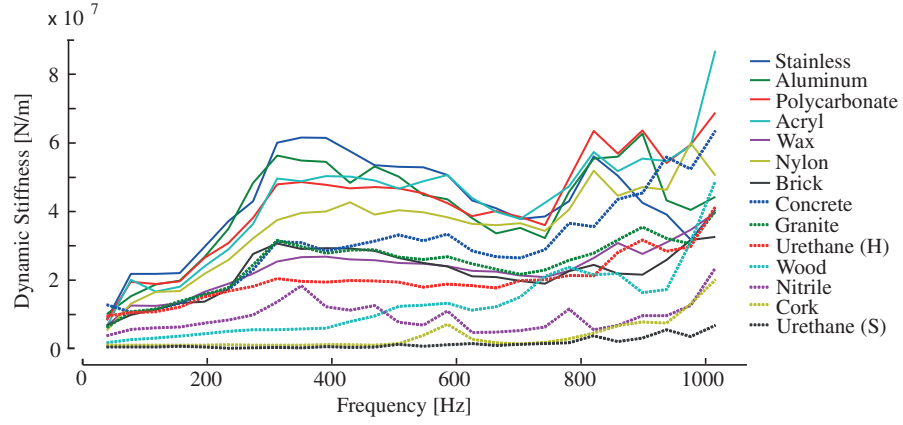


Fig. 5. Dynamic stiffness of the material specimens

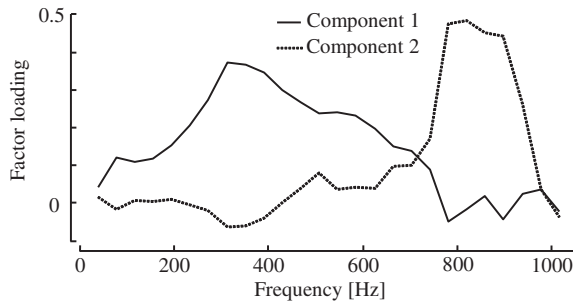


Fig. 6. Loading vectors of principal components. Loadings are scaled by using their eigenvalues.

be a product of \mathbf{A} and regression coefficients $\mathbf{z} \in \mathbb{R}^{n' \times 1}$ and determined by

$$\mathbf{h} = \mathbf{Az} + c. \quad (5)$$

Using the stepwise method, we selected the explanatory variables that significantly affect the objective variables. As a result, two of the three principal components that are shown in Fig. 6 were found to influence the hardness scores. Hence, finally, using the scores for these two components, the regression equation was determined to be

$$\mathbf{h} = \mathbf{A}_{12}\mathbf{z}_{12} + c \quad (6)$$

where $\mathbf{A}_{12} \in \mathbb{R}^{m \times 2}$ and $\mathbf{z}_{12} \in \mathbb{R}^{2 \times 1}$ are a submatrix of \mathbf{A} and corresponding regression coefficients, respectively. Above equation is identical to

$$\mathbf{h} = \mathbf{SB}_{12}^{-1}\mathbf{z}_{12} + c \quad (7)$$

where $\mathbf{B}_{12} \in \mathbb{R}^{2 \times n}$ included the two principal component vectors that significantly affected the hardness scores. Here, $\mathbf{w} = \mathbf{B}_{12}^{-1}\mathbf{z}_{12}$ is regarded as perceptual weights against the stiffness values for n representative frequencies.

D. Results

Fig. 6 shows the two principal components of dynamic stiffness involved in the regression analysis. One of the component displayed greater stiffness values at middle frequency

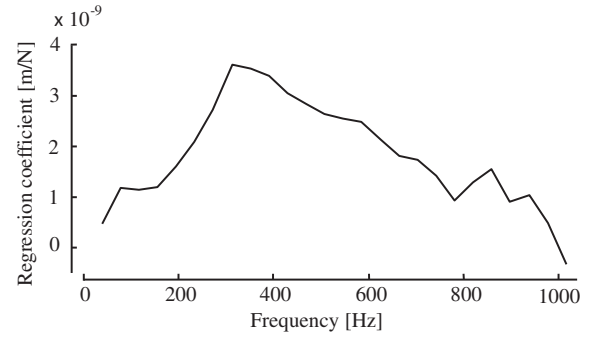


Fig. 7. Frequency characteristics of the weight function for the subjective hardness and dynamic stiffness

range with the peak value being around 300 Hz. The other component included larger stiffness values at high frequency range around 800 Hz.

Fig. 7 shows the perceptual weights (\mathbf{w}) on the dynamic stiffness values from 40–1,000 Hz. Except for 1,000 Hz, the weights were positive, which indicates that the greater stiffness values led to the greater hardness perception. The weight values differed across the frequency, suggesting that the perceptual effects of dynamic stiffness depend on the frequency. The stiffness values around 300 Hz were most weighted, and those at high frequencies decreased as the frequency increased. The constant value c in the regression equation was $c = -1.20$.

Fig. 8 compares the hardness scores observed by the participants and those estimated by the dynamic stiffness of objects using the regression model. The correlation coefficient between the observed and estimated scores was 0.93, and the regression model effectively represented the perceived hardness scores.

VI. DISCUSSION

From Fig. 8, the dynamic stiffness of the object was found to be an effective predictor for the hardness perceived by tapping. In other words, the hardness perception is likely to be based on the relationships between the force acted on the

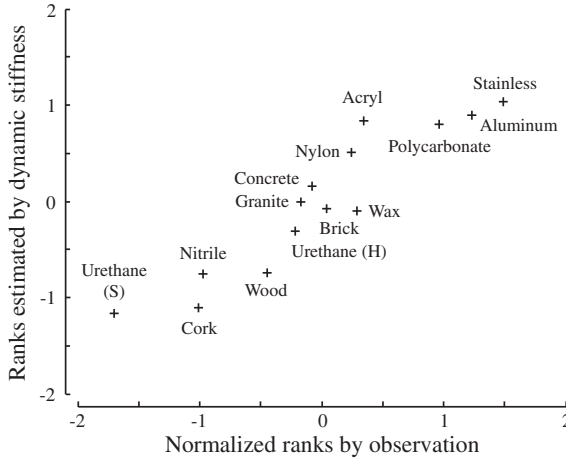


Fig. 8. Correlation between the observed and estimated hardness ranks.
 $r = 0.93$.

object surface and its surface vibration. In earlier studies using force or vibrotactile display devices, the reaction stimuli toward tapping were produced based on the contact speed or momentum of the virtual hand or tool [1], [2], [3], [4], [13], which was physically correct and perceptually effective in terms of the realism of virtual stimuli. Given that the momentum change of the virtual hand is identical to the impulse of the reaction force, it is natural for the human perception of contact events to be linked with the dynamic stiffness values that are defined by the ratio of the tapping force to reactive vibration amplitudes.

The weights on the stiffness values shown in Fig. 7 suggested that the effects of dynamic stiffness depends on the frequency. This may be due to the human vibrotactile characteristics that is also frequency-dependent. We should note that although multivariate analysis mathematically finds the best linkage between the human perception and the physical properties of the objects, their results do not always correctly reflect the characteristics of human perceptual system. Nonetheless, unequal contribution of dynamic stiffness across the wide frequency range is reasonable. The human vibrotactile sensitivity is highest around 250 Hz and deteriorates above this frequency [12]. At even higher range, the perception of vibrotactile stimuli is difficult. Such sensitivity largely agrees with the weights on dynamic stiffness shown in Fig. 7. The weights were maximum at approximately 300 Hz near which the vibrotactile perception is most sensitive. Above 900 Hz in which the vibrotactile perception is unlikely to operate, the weights were nearly zero and suggested that the stiffness values have no impact on hardness perception. These consistency between the characteristics of human vibrotactile perception and the weights of dynamic stiffness computed in the present study corroborates

their reasonable relationships, whereas further studies are necessary before being conclusive.

VII. CONCLUSION

To seek for the relationships between the wide-range dynamic characteristics of an object and the hardness perception by tapping, we linked their dynamic stiffness values and subjective hardness scores. We found that dynamic stiffness across 40–1,000 Hz effectively estimates the hardness perception. Their frequency-dependent contributions to the perception can be reasonably interpreted based on the vibrotactile characteristics of humans. These findings may lead to the design of frequency-filters or frequency-weighting-functions for vibrotactile rendering methods using display devices whose frequency responses are limited.

REFERENCES

- [1] A. M. Okamura, M. R. Cutkosky, and J. T. Dennerlein, “Reality-based models for vibration feedback in virtual environments,” *IEEE/ASME Transactions on Mechatronics*, vol. 6, no. 3, pp. 245–252, 2001.
- [2] K. J. Kuchenbecker, J. Fiene, and G. Niemeyer, “Improving contact realism through event-based haptic feedback,” *IEEE Transactions on Visualization and Computer Graphics*, vol. 12, no. 2, pp. 219–230, 2006.
- [3] Y. Ikeda and S. Hasegawa, “Characteristics of perception of stiffness by varied tapping velocity and penetration in using event-based haptic,” *Proceedings of 15th Joint Virtual Reality Eurographics Conference on Virtual Environments*, pp. 113–116, 2009.
- [4] K. Higashi, S. Okamoto, H. Nagano, and Y. Yamada, “Effects of mechanical parameters on hardness experienced by damped natural vibration stimulation,” *Proceedings of IEEE International Conference on Systems, Man, and Cybernetics*, pp. 1539–1544, 2015.
- [5] K. Higashi, S. Okamoto, H. Nagano, M. Konyo, and Y. Yamada, “Perceived hardness by tapping: The role of a secondary mode of vibration,” *Proceedings of AsiaHaptics 2016*, p. 4A-2, 2016.
- [6] K. Higashi, S. Okamoto, and Y. Yamada, “What is the hardness perceived by tapping?” in *Haptics: Perception, Devices, Control, and Applications*, ser. Lecture Notes in Computer Science, F. Bello, H. Kajimoto, and Y. Visell, Eds., vol. 9774. Springer, 2016, pp. 3–12.
- [7] D. A. Lawrence, L. Y. Pao, A. M. Dougherty, M. A. Salada, and Y. Pavlou, “Rate-hardness: A new performance metric for haptic interfaces,” *IEEE Transactions on Robotics and Automation*, vol. 16, no. 4, pp. 357–371, 2000.
- [8] G. Han and S. Choi, “Extended rate-hardness: a measure for perceived hardness,” *Proceedings of International Conference on Human Haptic Sensing and Touch Enabled Computer Applications*, pp. 117–124, 2010.
- [9] R. H. LaMotte, “Softness discrimination with a tool,” *Journal of Neurophysiology*, vol. 83, no. 4, pp. 1777–1786, 2000.
- [10] W. M. Bergmann Tiest and A. M. L. Kappers, “Cues for haptic perception of compliance,” *IEEE Transactions on Haptics*, vol. 2, no. 4, pp. 189–199, 2009.
- [11] H. L. Harter, “Expected values of normal order statistics,” *Biometrika*, vol. 48, no. 1, pp. 151–165, 1961.
- [12] S. J. Bolanowski Jr, G. A. Gescheider, R. T. Verrillo, and C. M. Checkosky, “Four channels mediate the mechanical aspects of touch,” *Journal of the Acoustical society of America*, vol. 84, no. 5, pp. 1680–1694, 1988.
- [13] H. Culbertson and K. J. Kuchenbecker, “Importance of matching physical friction, hardness, and texture in creating realistic haptic virtual surfaces,” *IEEE Transactions on Haptics*, vol. 10, no. 1, pp. 63–74, 2017.